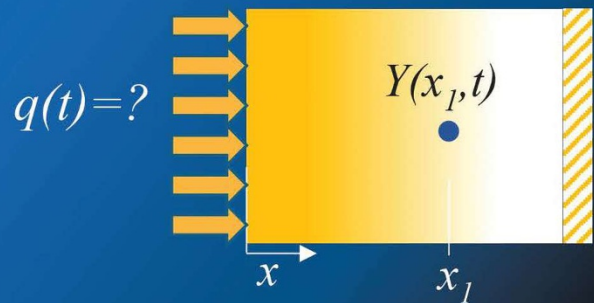


Second Edition

# Inverse Heat Conduction

Ill-Posed Problems

Keith A. Woodbury • Hamidreza Najafi  
Filippo de Monte • James V. Beck



$$\mathbf{q} = \mathbf{F}\mathbf{Y} \quad \leftarrow \quad \begin{aligned} \mathbf{T} &= \mathbf{X}\mathbf{q} \\ \mathbf{Y} &= \mathbf{T} + \boldsymbol{\varepsilon} \end{aligned}$$

WILEY



## Inverse Heat Conduction





# Inverse Heat Conduction

Ill-Posed Problems

Second Edition

*Keith A. Woodbury*  
*University of Alabama*  
*Tuscaloosa, AL, USA*

*Hamidreza Najafi*  
*Florida Institute of Technology*  
*Melbourne, FL, USA*

*Filippo de Monte*  
*University of L'Aquila*  
*L'Aquila, Italy*

*James V. Beck*  
*Michigan State University*  
*East Lansing, MI, USA*

**WILEY**

Copyright © 2023 by John Wiley & Sons, Inc. All rights reserved.

*Edition History*

First edition published in 1985

Published by John Wiley & Sons, Inc., Hoboken, New Jersey.

Published simultaneously in Canada.

No part of this publication may be reproduced, stored in a retrieval system, or transmitted in any form or by any means, electronic, mechanical, photocopying, recording, scanning, or otherwise, except as permitted under Section 107 or 108 of the 1976 United States Copyright Act, without either the prior written permission of the Publisher, or authorization through payment of the appropriate per-copy fee to the Copyright Clearance Center, Inc., 222 Rosewood Drive, Danvers, MA 01923, (978) 750-8400, fax (978) 750-4470, or on the web at [www.copyright.com](http://www.copyright.com).

Requests to the Publisher for permission should be addressed to the Permissions Department, John Wiley & Sons, Inc., 111 River Street, Hoboken, NJ 07030, (201) 748-6011, fax (201) 748-6008, or online at <http://www.wiley.com/go/permission>.

Trademarks: Wiley and the Wiley logo are trademarks or registered trademarks of John Wiley & Sons, Inc. and/or its affiliates in the United States and other countries and may not be used without written permission. All other trademarks are the property of their respective owners. John Wiley & Sons, Inc. is not associated with any product or vendor mentioned in this book.

*Limit of Liability/Disclaimer of Warranty*

While the publisher and author have used their best efforts in preparing this book, they make no representations or warranties with respect to the accuracy or completeness of the contents of this book and specifically disclaim any implied warranties of merchantability or fitness for a particular purpose. No warranty may be created or extended by sales representatives or written sales materials. The advice and strategies contained herein may not be suitable for your situation. You should consult with a professional where appropriate. Further, readers should be aware that websites listed in this work may have changed or disappeared between when this work was written and when it is read. Neither the publisher nor authors shall be liable for any loss of profit or any other commercial damages, including but not limited to special, incidental, consequential, or other damages.

For general information on our other products and services or for technical support, please contact our Customer Care Department within the United States at (800) 762-2974, outside the United States at (317) 572-3993 or fax (317) 572-4002.

Wiley also publishes its books in a variety of electronic formats. Some content that appears in print may not be available in electronic formats. For more information about Wiley products, visit our web site at [www.wiley.com](http://www.wiley.com).

***Library of Congress Cataloging-in-Publication Data:***

Names: Woodbury, Keith A., author. | Najafi, Hamidreza, author. | De Monte,

Filippo, author. | Beck, J. V. (James Vere), 1930– author.

Title: Inverse heat conduction : ill-posed problems / Keith Woodbury,

University of Alabama, Hamidreza Najafi, Florida Institute of

Technology, Filippo de Monte, University L'Aquila, James V. Beck,

Michigan State University.

Description: Second edition. | Hoboken, NJ : John Wiley & Sons, Inc., 2023.

| Preceded by: Inverse heat conduction / James V. Beck, Ben Blackwell,

Charles R. St. Clair, Jr. c1985. | Includes bibliographical references.

Identifiers: LCCN 2022039047 (print) | LCCN 2022039048 (ebook) | ISBN

9781119840190 (cloth) | ISBN 9781119840206 (adobe pdf) | ISBN

9781119840213 (epub)

Subjects: LCSH: Heat-Conduction. | Numerical analysis—Improperly posed problems.

Classification: LCC QC320 .B4 2023 (print) | LCC QC320 (ebook) | DDC

536/.23—dc23/eng20230106

LC record available at <https://lcn.loc.gov/2022039047>

LC ebook record available at <https://lcn.loc.gov/2022039048>

Cover Design: Wiley

Cover Images: © AnitaVDB/Getty Images; bischy/Getty Images; Bernt Ove Moss/Getty Images; SasinT Gallery/Getty Images;

Courtesy of Hamidreza Najafi

Set in 9.5/12.5pt STIXTwoText by Straive, Pondicherry, India

*To engineers and researchers who thirst for knowledge and pass this way, with undying gratitude for those who came before and illuminated the path, and with special appreciation to my colleague, mentor, and co-author: James V. Beck.*

*K. A. W.*

*To my wife, Mehrasa; and to my mother and father, Kobra and Mohammadsadegh.*

*H. N.*

*To my wife Emanuela and my children Federica Flora, Matilde, and Fabrizio Nicola; to my sisters Saveria and Alessia.*

*F. d. M.*

*To my wife, Barbara; children, Sharon and Douglas; and father and mother, Peter and Louise Beck*

*J. V. B.*

### **In Memorium**

James V. Beck (1930–2022)

Prof. Beck was the inspirational and motivational force in the development of the two editions of *Inverse Heat Conduction: Ill-posed problems*. Sadly, he passed away during the last stages of copyediting of this second edition. His spirited enthusiasm and boundless energy for scientific research will not soon be forgotten.

## Contents

<b>List of Figures</b>	<i>xv</i>
<b>Nomenclature</b>	<i>xxi</i>
<b>Preface to First Edition</b>	<i>xxvi</i>
<b>Preface to Second Edition</b>	<i>xxvii</i>
<b>1</b>	<b>Inverse Heat Conduction Problems: An Overview 1</b>
1.1	Introduction 1
1.2	Basic Mathematical Description 3
1.3	Classification of Methods 4
1.4	Function Estimation Versus Parameter Estimation 5
1.5	Other Inverse Function Estimation Problems 6
1.6	Early Works on IHCPs 7
1.7	Applications of IHCPs: A Modern Look 7
1.7.1	Manufacturing Processes 7
1.7.1.1	Machining Processes 7
1.7.1.2	Milling and Hot Forming 9
1.7.1.3	Quenching and Spray Cooling 9
1.7.1.4	Jet Impingement 11
1.7.1.5	Other Manufacturing Applications 11
1.7.2	Aerospace Applications 11
1.7.3	Biomedical Applications 12
1.7.4	Electronics Cooling 13
1.7.5	Instrumentation, Measurement, and Non-Destructive Testing 13
1.7.6	Other Applications 14
1.8	Measurements 15
1.8.1	Description of Measurement Errors 15
1.8.2	Statistical Description of Errors 15
1.9	Criteria for Evaluation of IHCP Methods 17
1.10	Scope of Book 17
1.11	Chapter Summary 18
	References 18
<b>2</b>	<b>Analytical Solutions of Direct Heat Conduction Problems 25</b>
2.1	Introduction 25
2.2	Numbering System 26
2.3	One-Dimensional Temperature Solutions 26
2.3.1	Generalized One-Dimensional Heat Transfer Problem 26
2.3.2	Cases of Interest 27
2.3.3	Dimensionless Variables 28
2.3.4	Exact Analytical Solution 28
2.3.5	The Concept of Computational Analytical Solution 29

2.3.5.1	Absolute and Relative Errors	30
2.3.5.2	Deviation Time	31
2.3.5.3	Second Deviation Time	31
2.3.5.4	Quasi-Steady, Steady-State and Unsteady Times	32
2.3.5.5	Solution for Large Times	32
2.3.5.6	Intrinsic Verification	33
2.3.6	X12B10T0 Case	33
2.3.6.1	Computational Analytical Solution	34
2.3.6.2	Computer Code and Plots	34
2.3.7	X12B20T0 Case	34
2.3.7.1	Computational Analytical Solution	36
2.3.7.2	Computer Code and Plots	36
2.3.8	X22B10T0 Case	37
2.3.8.1	Computational Analytical Solution	38
2.3.8.2	Computer Code and Plots	39
2.3.9	X22B20T0 Case	40
2.3.9.1	Computational Analytical Solution	40
2.3.9.2	Computer Code and Plots	41
2.4	Two-Dimensional Temperature Solutions	42
2.4.1	Dimensionless Variables	43
2.4.2	Exact Analytical Solution	43
2.4.3	Computational Analytical Solution	44
2.4.3.1	Absolute and Relative Errors	45
2.4.3.2	One- and Two-Dimensional Deviation Times	46
2.4.3.3	Quasi-Steady Time	48
2.4.3.4	Number of Terms in the Quasi-Steady Solution with Eigenvalues in the Homogeneous Direction	50
2.4.3.5	Number of Terms in the Quasi-Steady Solution with Eigenvalues in the Nonhomogeneous Direction	50
2.4.3.6	Deviation Distance Along $x$	51
2.4.3.7	Deviation Distance Along $y$	53
2.4.3.8	Number of Terms in the Complementary Transient Solution	54
2.4.3.9	Computer Code and Plots	56
2.5	Chapter Summary	57
	Problems	58
	References	59
<b>3</b>	<b>Approximate Methods for Direct Heat Conduction Problems</b>	<b>61</b>
3.1	Introduction	61
3.1.1	Various Numerical Approaches	61
3.1.2	Scope of Chapter	61
3.2	Superposition Principles	62
3.2.1	Green's Function Solution Interpretation	63
3.2.2	Superposition Example – Step Pulse Heating	63
3.3	One-Dimensional Problem with Time-Dependent Surface Temperature	64
3.3.1	Piecewise-Constant Approximation	64
3.3.1.1	Superposition-Based Numerical Approximation of the Solution	65
3.3.1.2	Sequential-in-time Nature and Sensitivity Coefficients	65
3.3.1.3	Basic “Building Block” Solution	66
3.3.1.4	Computer Code and Example	66
3.3.1.5	Matrix Form of the Superposition-Based Numerical Approximation	68
3.3.2	Piecewise-Linear Approximation	69
3.3.2.1	Superposition-Based Numerical Approximation of the Solution	70
3.3.2.2	Sequential-in-time Nature and Sensitivity Coefficients	71
3.3.2.3	Basic “Building Block” Solutions	72
3.3.2.4	Computer Code and Examples	72

3.3.2.5	Matrix Form of the Superposition-Based Numerical Approximation	74
3.4	One-Dimensional Problem with Time-Dependent Surface Heat Flux	75
3.4.1	Piecewise-Constant Approximation	76
3.4.1.1	Superposition-Based Numerical Approximation of the Solution	76
3.4.1.2	Heat Flux-Based Sensitivity Coefficients	77
3.4.1.3	Basic “Building Block” Solution	77
3.4.1.4	Computer Code and Example	77
3.4.1.5	Matrix Form of the Superposition-Based Numerical Approximation	79
3.4.2	Piecewise-Linear Approximation	79
3.4.2.1	Superposition-Based Numerical Approximation of the Solution	81
3.4.2.2	Heat Flux-Based Sensitivity Coefficients	81
3.4.2.3	Basic “Building Block” Solutions	82
3.4.2.4	Computer Code and Examples	82
3.4.2.5	Matrix Form of the Superposition-Based Numerical Approximation	84
3.5	Two-Dimensional Problem with Space-Dependent and Constant Surface Heat Flux	85
3.5.1	Piecewise-Uniform Approximation	85
3.5.1.1	Superposition-Based Numerical Approximation of the Solution	87
3.5.1.2	Heat Flux-Based Sensitivity Coefficients	87
3.5.1.3	Basic “Building Block” Solution	87
3.5.1.4	Computer Code and Examples	88
3.5.1.5	Matrix Form of the Superposition-Based Numerical Approximation	90
3.6	Two-Dimensional Problem with Space- and Time-Dependent Surface Heat Flux	90
3.6.1	Piecewise-Uniform Approximation	91
3.6.1.1	Numerical Approximation in Space	91
3.6.2	Piecewise-Constant Approximation	91
3.6.2.1	Numerical Approximation in Time	92
3.6.3	Superposition-Based Numerical Approximation of the Solution	92
3.6.3.1	Sequential-in-time Nature and Sensitivity Coefficients	94
3.6.3.2	Basic “Building Block” Solution	95
3.6.3.3	Computer Code and Example	95
3.6.3.4	Matrix Form of the Superposition-Based Numerical Approximation	97
3.7	Chapter Summary	98
	Problems	99
	References	101
<b>4</b>	<b>Inverse Heat Conduction Estimation Procedures</b>	<b>103</b>
4.1	Introduction	103
4.2	Why is the IHCP Difficult?	104
4.2.1	Sensitivity to Errors	104
4.2.2	Damping and Lagging	104
4.2.2.1	Penetration Time	104
4.2.2.2	Importance of the Penetration Time	105
4.3	Ill-Posed Problems	105
4.3.1	An Exact Solution	105
4.3.2	Discrete System of Equations	107
4.3.3	The Need for Regularization	108
4.4	IHCP Solution Methodology	108
4.5	Sensitivity Coefficients	108
4.5.1	Definition of Sensitivity Coefficients and Linearity	108
4.5.2	One-Dimensional Sensitivity Coefficient Examples	110
4.5.2.1	X22 Plate Insulated on One Side	110
4.5.2.2	X12 Plate Insulated on One Side, Fixed Boundary Temperature	113
4.5.2.3	X32 Plate Insulated on One Side, Fixed Heat Transfer Coefficient	113

4.5.3	Two-Dimensional Sensitivity Coefficient Example	114
4.6	Stolz Method: Single Future Time Step Method	116
4.6.1	Introduction	116
4.6.2	Exact Matching of Measured Temperatures	116
4.7	Function Specification Method	118
4.7.1	Introduction	118
4.7.2	Sequential Function Specification Method	119
4.7.2.1	Piecewise Constant Functional Form	119
4.7.2.2	Piecewise Linear Functional Form	125
4.7.3	General Remarks About Function Specification Method	127
4.8	Tikhonov Regularization Method	127
4.8.1	Introduction	127
4.8.2	Physical Significance of Regularization Terms	128
4.8.2.1	Continuous Formulation	128
4.8.2.2	Discrete Formulation	128
4.8.3	Whole Domain TR Method	129
4.8.3.1	Matrix Formulation	129
4.8.4	Sequential TR Method	133
4.8.5	General Comments About Tikhonov Regularization	134
4.9	Gradient Methods	134
4.9.1	Conjugate Gradient Method	134
4.9.1.1	Fletcher-Reeves CGM	136
4.9.1.2	Polak-Ribiere CGM	136
4.9.2	Adjoint Method (Nonlinear Problems)	137
4.9.2.1	Some Necessary Mathematics	138
4.9.2.2	The Continuous Form of IHCP	139
4.9.2.3	The Sensitivity Problem	139
4.9.2.4	The Lagrangian and the Adjoint Problem	140
4.9.2.5	The Gradient Equation	141
4.9.2.6	Summary of IHCP solution by Adjoint Method	142
4.9.2.7	Comments About Adjoint Method	142
4.9.3	General Comments about CGM	143
4.10	Truncated Singular Value Decomposition Method	143
4.10.1	SVD Concepts	143
4.10.2	TSVD in the IHCP	144
4.10.3	General Remarks About TSVD	145
4.11	Kalman Filter	145
4.11.1	Discrete Kalman Filter	146
4.11.2	Two Concepts for Applying Kalman Filter to IHCP	147
4.11.3	Scarpa and Milano Approach	148
4.11.3.1	Kalman Filter	148
4.11.3.2	Smoother	149
4.11.4	General Remarks About Kalman Filtering	150
4.12	Chapter Summary	150
	Problems	151
	References	154
<b>5</b>	<b>Filter Form of IHCP Solution</b>	<b>157</b>
5.1	Introduction	157
5.2	Temperature Perturbation Approach	157
5.3	Filter Matrix Perspective	159
5.3.1	Function Specification Method	159
5.3.2	Tikhonov Regularization	161



5.3.3	Singular Value Decomposition	162
5.3.4	Conjugate Gradient	163
5.4	Sequential Filter Form	164
5.5	Using Second Temperature Sensor as Boundary Condition	166
5.5.1	Exact Solution for the Direct Problem	166
5.5.2	Tikhonov Regularization Method as IHCP Solution	168
5.5.3	Filter Form of IHCP Solution	168
5.6	Filter Coefficients for Multi-Layer Domain	171
5.6.1	Solution Strategy for IHCP in Multi-Layer Domain	171
5.6.1.1	Inner Layer	171
5.6.1.2	Outer Layer	172
5.6.1.3	Combined Solution	173
5.6.2	Filter Form of the Solution	173
5.7	Filter Coefficients for Non-Linear IHCP: Application for Heat Flux Measurement Using Directional Flame Thermometer	174
5.7.1	Solution for the IHCP	176
5.7.1.1	Back Layer (Insulation)	176
5.7.1.2	Front Layer (Inconel plate)	176
5.7.1.3	Combined Solution	176
5.7.2	Filter form of the solution	177
5.7.3	Accounting for Temperature-Dependent Material Properties	177
5.7.4	Examples	179
5.8	Chapter Summary	183
	Problems	184
	References	184
<b>6</b>	<b>Optimal Regularization</b>	<b>187</b>
6.1	Preliminaries	187
6.1.1	Some Mathematics	187
6.1.2	Design vs. Experimental Setting	188
6.2	Two Conflicting Objectives	188
6.2.1	Minimum Deterministic Bias	188
6.2.2	Minimum Sensitivity to Random Errors	188
6.2.3	Balancing Bias and Variance	189
6.3	Mean Squared Error	189
6.4	Minimize Mean Squared Error in Heat Flux $R_q^2$	190
6.4.1	Definition of $R_q^2$	190
6.4.2	Expected Value of $R_q^2$	191
6.4.3	Optimal Regularization Using $E(R_q^2)$	193
6.5	Minimize Mean Squared Error in Temperature $R_T^2$	196
6.5.1	Definition of $R_T^2$	196
6.5.2	Expected Value of $R_T^2$	197
6.5.3	Morozov Discrepancy Principle	197
6.6	The L-Curve	199
6.6.1	Definition of L-Curve	199
6.6.2	Using Expected Value to Define L-Curve	199
6.6.3	Optimal Regularization Using L-Curve	200
6.7	Generalized Cross Validation	201
6.7.1	The GCV Function	202
6.8	Chapter Summary	205
	Problems	205
	References	206

<b>7</b>	<b>Evaluation of IHCP Solution Procedures</b>	<b>209</b>
7.1	Introduction	209
7.2	Test Cases	210
7.2.1	Introduction	210
7.2.2	Step Change in Surface Heat Flux	211
7.2.3	Triangular Heat Flux	211
7.2.4	Quartic Heat Flux	213
7.2.5	Random Errors	216
7.2.6	Temperature Perturbation	217
7.2.7	Test Cases with Units	217
7.3	Function Specification Method	217
7.3.1	Step Change in Surface Heat Flux	218
7.3.2	Triangular Heat Flux	219
7.3.3	Quartic Heat Flux	219
7.3.4	Temperature Perturbation	221
7.3.5	Function Specification Test Case Summary	223
7.4	Tikhonov Regularization	224
7.4.1	Step Change in Surface Heat Flux	224
7.4.2	Triangular Heat Flux and Quartic Heat Flux	225
7.4.3	Temperature Perturbation	226
7.4.4	Tikhonov Regularization Test Case Summary	228
7.5	Conjugate Gradient Method	229
7.5.1	Step Change in Surface Heat Flux	229
7.5.2	Triangular Heat Flux and Quartic Heat Flux	230
7.5.3	Temperature Perturbation	232
7.5.4	Conjugate Gradient Test Case Summary	234
7.6	Truncated Singular Value Decomposition	234
7.6.1	Step Change in Surface Heat Flux	235
7.6.2	Triangular and Quartic Heat Flux	236
7.6.3	Temperature Perturbation	237
7.6.4	TSVD Test Case Summary	238
7.7	Kalman Filter	239
7.7.1	Step Change in Surface Heat Flux	239
7.7.2	Triangular and Quartic Heat Flux	239
7.7.3	Temperature Perturbation	241
7.7.4	Kalman Filter Test Case Summary	244
7.8	Chapter Summary	245
	Problems	247
	References	248
<b>8</b>	<b>Multiple Heat Flux Estimation</b>	<b>249</b>
8.1	Introduction	249
8.2	The Forward and the Inverse Problems	249
8.2.1	Forward Problem	249
8.2.2	Inverse Problem	250
8.2.3	Filter Form of the Solution	251
8.3	Examples	254
8.4	Chapter Summary	258
	Problems	258
	References	259

<b>9</b>	<b>Heat Transfer Coefficient Estimation</b>	<b>261</b>
9.1	Introduction	261
9.1.1	Recent Literature	261
9.1.2	Basic Approach	262
9.2	Sensitivity Coefficients	263
9.3	Lumped Body Analyses	266
9.3.1	Exact Matching of the Measured Temperatures	266
9.3.2	Filter Coefficient Solution	268
9.3.3	Estimating Constant Heat Transfer Coefficient	269
9.4	Bodies with Internal Temperature Gradients	272
9.5	Chapter Summary	274
	Problems	274
	References	275
<b>10</b>	<b>Temperature Measurement</b>	<b>277</b>
10.1	Introduction	277
10.1.1	Subsurface Temperature Measurement	277
10.1.2	Surface Temperature Measurement	278
10.2	Correction Kernel Concept	278
10.2.1	Direct Calculation of Surface Heat Flux	278
10.2.2	Temperature Correction Kernels	279
10.2.2.1	Determining the Correction Kernel	279
10.2.2.2	Correcting Temperature Measurements	280
10.2.3	2-D Axisymmetric Model	280
10.2.4	High Fidelity Models and Thermocouple Measurement	285
10.2.4.1	Three-Dimensional Models	285
10.2.4.2	Location of Sensed Temperature in Thermocouples	286
10.2.5	Experimental Determination of Sensitivity Function	286
10.3	Unsteady Surface Element Method	287
10.3.1	Intrinsic Thermocouple	288
10.4	Chapter Summary	291
	Problems	292
	References	293
	<b>Appendix A Numbering System</b>	<b>295</b>
	<b>Appendix B Exact Solution</b>	<b>301</b>
	<b>Appendix C Green's Functions Solution Equation</b>	<b>309</b>
	<b>Index</b>	<b>321</b>



## List of Figures

- Figure 1.1** Schematic of 1D slab subject to heat flux at  $x = 0$ . (a) Direct heat conduction problem. (b) Inverse heat conduction problem (IHCP). 2
- Figure 1.2** (a) Measured temperatures at discrete times. (b) Representations of calculated surface heat fluxes. 2
- Figure 1.3** Subdivision of a single interior sensor IHCP into inverse and direct problems. 4
- Figure 1.4** Composite plate with multiple temperature sensors. 4
- Figure 1.5** Surface heat flux as a function of position for a flat plate. 7
- Figure 1.6** Examples of studies involving solution of IHCP in manufacturing. (a) Metal cutting (b) Laser assisted machining. 8
- Figure 1.7** Examples of studies involving solution of IHCP in manufacturing. (a) Hot forming. (b) Hryogenic quenching. 10
- Figure 1.8** Example of reentering vehicle for which the surface heat flux is needed. (a) Reentering vehicle schematic; (b) Section A. 11
- Figure 1.9** Schematic of a three-layer thermal protection system. 12
- Figure 2.1** Schematic of the 1D transient X32B-0T1 problem. 27
- Figure 2.2** Nonhomogeneous constant boundary condition of the first kind at  $x = 0$  for a slab initially at  $T_{in}$  and insulated on the back side  $x = L$ : (a) dimensional (X12B10T1); and (b) dimensionless (X12B10T0). 33
- Figure 2.3** Dimensionless temperature of the X12B10T0 problem: (a) versus space with time as a parameter; (b) as a function of time for different locations. 35
- Figure 2.4** Nonhomogeneous linearly-in-time variable boundary condition of the first kind at  $x = 0$  for a slab initially at  $T_{in}$  and insulated on the back side  $x = L$ : (a) dimensional (X12B20T1); and (b) dimensionless (X12B20T0). 35
- Figure 2.5** Dimensionless temperature of the X12B20T0 problem for  $\tilde{t}_{ref} = 1$ : (a) versus space with time as a parameter; (b) as a function of time for different locations. 37
- Figure 2.6** Nonhomogeneous constant boundary condition of the second kind at  $x = 0$  for a slab initially at  $T_{in}$  and insulated on the back side  $x = L$ : (a) dimensional (X22B10T1); and (b) dimensionless (X22B10T0). 38
- Figure 2.7** Dimensionless temperature of the X22B10T0 problem: (a) versus space with time as a parameter; (b) as a function of time for different locations. 39
- Figure 2.8** Nonhomogeneous linearly-in-time variable boundary condition of the second kind at  $x = 0$  for a slab initially at  $T_{in}$  and insulated on the back side: (a) dimensional (X22B20T1); and (b) dimensionless (X22B20T0). 40
- Figure 2.9** Dimensionless temperature of the X22B20T0 problem for  $\tilde{t}_{ref} = 1$ : (a) versus space with time as a parameter; (b) as a function of time for different locations. 42
- Figure 2.10** Schematic of the 2D transient X22B(y1pt1)0Y22B00T1 problem. 42
- Figure 2.11** Dimensionless temperature of the X22B(y1pt1)0Y22B00T0 problem versus  $\tilde{x}$  with  $\tilde{y}$  as a parameter when  $\tilde{W} = 1$  and  $\tilde{W}_0 = \tilde{W}/2$ : (a) at time  $\tilde{t} = 0.25$ ; (b) at time  $\tilde{t} = 0.5$ . 56
- Figure 3.1** Piecewise-constant approximation for  $\theta_0(t)$  where the  $i$ th component,  $\theta_{0,i}$ , is time independent. 64
- Figure 3.2** Component “ $i$ ” of the piecewise-constant approximation for the surface temperature rise over the time interval  $t = (i - 1)\Delta t \rightarrow i\Delta t$ . 65
- Figure 3.3** Piecewise-linear approximation for  $\theta_0(t)$  where the  $i$ th component,  $\theta_{0,i}$ , varies linearly with time. 69
- Figure 3.4** Component “ $i$ ” of the piecewise-linear approximation for the surface temperature rise defined by Eq. (3.25)–(3.26c). 70

- Figure 3.5** Plot of exact and approximate variations of the surface temperature into the range  $t \in [0, 5 \text{ s}]$  when dealing with  $\Delta t = 5 \text{ s}$ . 74
- Figure 3.6** Piecewise-constant approximation for  $q_0(t)$  where the  $i$ th component,  $q_{0,i}$ , is time-independent. 76
- Figure 3.7** Piecewise-linear approximation for  $q_0(t)$  where the  $i$ th component,  $q_{0,i}$ , changes linearly with time. 80
- Figure 3.8** Plot of exact and approximate variations of the surface heat flux into the range  $t \in [0, 5 \text{ s}]$  when dealing with  $\Delta t = 5 \text{ s}$ . 84
- Figure 3.9** Piecewise-uniform approximation for the surface heat flux where the  $j$ th component,  $q_{0,j}$ , is space-independent. 86
- Figure 3.10** Superposition in space applied to the  $T_j(x, y, t)$  temperature due to the  $q_{0,j}$  heat flux component. 86
- Figure 3.11** Building blocks differences: (a) backward difference (BD) in space; (b) forward difference (FD) in time; (c) second cross difference in both space and time. 93
- Figure 4.1** Piecewise constant (dashed lines) and piecewise linear approximations (solid lines and circles) to heat flux history. 109
- Figure 4.2** Heat flux sensitivity coefficients at insulated surface of flat plate for piecewise constant heat flux model. 112
- Figure 4.3** Heat flux sensitivity coefficients at insulated surface of flat plate for piecewise linear heat flux model. 112
- Figure 4.4** Sensitivity coefficients for temperature (X12) compared to those for heat flux (X22). 113
- Figure 4.5** Sensitivity coefficients for estimating a constant Bi for Bi = 1, 10, and 100.  $x_s = L$ . 114
- Figure 4.6** Finite two-dimensional slab with piecewise constant heat flux pulses at time  $t_i$ . 114
- Figure 4.7** Two-dimensional sensitivity coefficients (a)  $W/L = 4$  and (b)  $W/L = 16$ . 115
- Figure 4.8** Scarpa and Milano results for varying process noise parameter. No smoothing is applied ( $r = 0$ ).  $\sigma_{\text{noise}} = 0.0025$ . 149
- Figure 4.9** Effect of post-Kalman estimation smoothing on estimated heat flux. (a) Optimal value of  $R_q = 42$ ,  $r = 0$  gives minimum RMS error in heat flux. (b) Smoothing with  $r = 7$  reduces RMS error in heat flux to new minimum.  $\sigma_{\text{noise}} = 0.0025$ . 150
- Figure 5.1** Columns 7–15 of the filter matrix for function specification method ( $\tilde{x} = 0.5$ ,  $\Delta\tilde{t} = 0.05$ , and  $r = 7$ ). 159
- Figure 5.2** Surface plot of the filter coefficients for the function specification method ( $\tilde{x} = 0.5$ ,  $\Delta\tilde{t} = 0.05$ , and  $r = 7$ ). 160
- Figure 5.3** Filter coefficients for zeroth order Tikhonov regularization ( $\tilde{x} = 0.5$ ,  $\Delta\tilde{t} = 0.05$  and  $\alpha_t = 0.001$ ). 161
- Figure 5.4** Surface plot of the rows of the filter matrix for Tikhonov regularization method ( $\tilde{x} = 0.5$ ,  $\Delta\tilde{t} = 0.05$ , and  $\alpha_t = 0.001$ ). 162
- Figure 5.5** Values of the filter coefficients along the main diagonal, diagonal +1 and diagonal –1 for singular value decomposition ( $\tilde{x} = 0.5$  for 31 time steps and 15 eigenvalues). 163
- Figure 5.6** Filter coefficients for the mid column and plus and minus 2 adjacent ones for the SVD method ( $\tilde{x} = 0.5$  for 31 time steps and 15 eigenvalues). 163
- Figure 5.7** Surface plot of the rows of the filter matrix for SVD method ( $\tilde{x} = 0.5$  for 31 time steps and 15 eigenvalues). 163
- Figure 5.8** Filter coefficients for the mid-column and plus and minus 1 adjacent columns for the CGM using Fletcher–Reeves algorithm ( $\tilde{x} = 0.5$ ,  $\Delta\tilde{t} = 0.05$ ). 163
- Figure 5.9** Surface plot of the columns of the CGM filter matrix ( $\tilde{x} = 0.5$ ,  $\Delta\tilde{t} = 0.05$  for 31 time steps). 164
- Figure 5.10** Mid-column of the TR-filter matrix for various dimensionless locations. 165
- Figure 5.11** Temperature response for X22B10T0 case at mid-plane ( $\tilde{x} = 0.5$  and  $\Delta\tilde{t} = 0.02$ ). 166
- Figure 5.12** Calculated surface heat flux using filter-based TR versus exact values ( $\tilde{x} = 0.5$ ,  $\Delta\tilde{t} = 0.02$  and  $\alpha = 0.0001$ ). 166
- Figure 5.13** Schematic of the physical domain with second temperature sensor as boundary condition. 167
- Figure 5.14** Dimensionless filter coefficients  $f$  for the surface heat flux at  $x = 0$  for different sensor locations. First-order Tikhonov regularization  $\alpha_T = 1\text{e-}4$  and  $\Delta\tilde{t} = 0.02$ . 169
- Figure 5.15** Dimensionless filter coefficients  $g$  for the surface heat flux at  $x = 0$  for different sensor locations. First-order Tikhonov regularization  $\alpha_T = 1\text{e-}4$  and  $\Delta\tilde{t} = 0.02$ . 169
- Figure 5.16** Temperatures for triangular heat flux profile ( $\Delta\tilde{t} = 0.02$ ). 170
- Figure 5.17** Comparison of estimated surface heat flux values by the whole-time domain TR and filter-based TR versus exact heat flux values ( $\Delta\tilde{t} = 0.02$ ,  $\alpha_T = 0.01$ ). 170

<b>Figure 5.18</b>	Schematic of the IHCP in a two-layer medium. 171
<b>Figure 5.19</b>	Dimensionless temperature for X1C11B10T0 case ( $t_d = 0.01$ ). 174
<b>Figure 5.20</b>	$f$ filter coefficients for the two-layer domain (X1C11B10T0, $t_d = 0.01$ , $\alpha_t = 0.005$ ). 174
<b>Figure 5.21</b>	$g$ filter coefficients for the two-layer domain (X1C11B10T0, $t_d = 0.01$ , $\alpha_t = 0.005$ ). 175
<b>Figure 5.22</b>	Calculated surface heat flux for (X1C11B10T0, $t_d = 0.01$ , $\alpha_t = 0.005$ ). 175
<b>Figure 5.23</b>	Schematic of a directional flame thermometer (DFT). 175
<b>Figure 5.24</b>	The two-layer IHCP associated with DFT application. 176
<b>Figure 5.25</b>	$f$ filter coefficients for different temperatures. 178
<b>Figure 5.26</b>	$g$ filter coefficients for different temperatures. 178
<b>Figure 5.27</b>	Temperature measurements on front ( <b>Y</b> ) and back ( <b>y</b> ) side of the second layer (Example 5.4). 180
<b>Figure 5.28</b>	Surface heat flux evaluated for 5.2 with constant material properties at different temperatures (sampling time: 1s, $m_p = 40$ , $m_f = 4$ , $\alpha_t = 10^{-2}$ ). 180
<b>Figure 5.29</b>	Calculated surface heat flux for Example 5.2 accounting for temperature dependent material properties (non-linear filter), ANSYS inputs and filter coefficients for constant material properties at average temperature of 691 K (sampling time: 1 seconds, $m_p = 150$ , $m_f = 8$ , $\alpha_t = 10^{-2}$ ). 181
<b>Figure 5.30</b>	Temperature measurement data for DFT field test (Example 5.5) 182
<b>Figure 5.31</b>	Calculated surface heat flux for DFT field data-constant material properties at different temperatures (sampling time: 5 seconds, $m_p = 40$ , $m_f = 4$ , $\alpha_t = 10^{-7}$ ). 182
<b>Figure 5.32</b>	Comparison of calculated surface heat flux for DFT field data by accounting for temperature dependent material properties (non-linear filter), constant material properties at the average temperature of 1049 K and results from IHCP1D whole time analysis (sampling time: 5 seconds, $m_p = 40$ , $m_f = 4$ , $\alpha_t = 10^{-7}$ ). 183
<b>Figure 6.1</b>	The true heat flux $q_M$ at time $t_M$ , the estimated value $\hat{q}_M$ , and the mean of the estimated value, $E(\hat{q}_M)$ . 190
<b>Figure 6.2</b>	Expected value of the average sum-squared error in heat flux with random and bias components for base case of Example 6.2. 194
<b>Figure 6.3</b>	Expected value of the average sum-squared error in heat flux with random and bias components for triangular heat flux case of Example 6.3. 196
<b>Figure 6.4</b>	Comparison of results from three regularization techniques applied to Example 6.4. 198
<b>Figure 6.5</b>	Histogram of results from 200 trials using the Discrepancy Principle on different sets of random Gaussian error in Example 6.4 (ET_IHCP_Tik.m, fig4). 198
<b>Figure 6.6</b>	Typical L-curve for 1-D IHCP. 200
<b>Figure 6.7</b>	Various “optimal” regularizations presented on the L-curves of Figure 6.6. 201
<b>Figure 6.8</b>	GCV function values for SVD regularization in Example 6.6. 203
<b>Figure 6.9</b>	GCV function values for CGM regularization in Example 6.6. 204
<b>Figure 7.1</b>	Various geometries, boundary conditions, and interface conditions that can be treated using superposition and convolution. Thermal properties are independent of temperature, (a), composite plate; (b) composite cylinder or sphere; (c) composite body of irregular shape; (d) axisymmetric semi-infinite body with cylindrical void and surface partially heated. 210
<b>Figure 7.2</b>	Heat flux test case for a step change in surface heat flux. 211
<b>Figure 7.3</b>	Triangular heat flux for test case. Finite insulated plate. 212
<b>Figure 7.4</b>	Heated and insulated surface temperatures for triangular heat flux test case. 212
<b>Figure 7.5</b>	Quartic heat flux pulse for test case. Finite insulated plate. 213
<b>Figure 7.6</b>	Heated and insulated surface temperatures for quartic heat flux pulse test case. 214
<b>Figure 7.7</b>	Estimated heat fluxes using function specification for step change test case with $\Delta\tilde{t} = 0.06$ using either piecewise constant or piecewise linear assumptions. 218
<b>Figure 7.8</b>	Estimated heat fluxes using function specification for step change test case with $\Delta\tilde{t} = 0.03$ using either piecewise constant or piecewise linear assumptions. 218
<b>Figure 7.9</b>	Estimated heat fluxes using function specification for triangular test case with $\Delta\tilde{t} = 0.06$ using either piecewise constant or piecewise linear assumptions. 219
<b>Figure 7.10</b>	Estimated heat fluxes using function specification for triangular test case with $\Delta\tilde{t} = 0.03$ using either piecewise constant or piecewise linear assumptions. 220

- Figure 7.11** Estimated heat fluxes using function specification for quartic test case with  $\Delta\tilde{t} = 0.06$  using either piecewise constant or piecewise linear assumptions. 220
- Figure 7.12** Estimated heat fluxes using function specification for quartic test case with  $\Delta\tilde{t} = 0.03$  using either piecewise constant or piecewise linear assumptions. 221
- Figure 7.13** Filter coefficients for function specification obtained from temperature perturbation case with  $\Delta\tilde{t} = 0.06$  using either piecewise constant or piecewise linear assumptions.  $r_{opt} = 4$  is shown which is optimal for step, triangular, and quartic cases using noisy data with  $\sigma_{noise} = 0.5\% \times T_{max}$ . 222
- Figure 7.14** Filter coefficients for function specification obtained from temperature perturbation case with  $\Delta\tilde{t} = 0.03$  using either piecewise constant or piecewise linear assumptions.  $r_{opt} = 6$  and  $r_{opt} = 8$  are shown. Optimal for step, triangular, and quartic cases using noisy data with  $\sigma_{noise} = 0.5\% \times T_{max}$  is  $7 \leq r_{opt} \leq 9$ . 222
- Figure 7.15** Filter coefficients for function specification obtained from temperature perturbation case with  $\Delta\tilde{t} = 0.06$  using piecewise linear assumption.  $r = 3, 4, 5$  are shown. 223
- Figure 7.16** Filter coefficients for function specification obtained from temperature perturbation case with  $\Delta\tilde{t} = 0.03$  using piecewise constant assumption.  $r = 6, 7, 8, 9$  are shown. 223
- Figure 7.17** Optimal estimated heat fluxes using Tikhonov Regularization for step change test case with  $\Delta\tilde{t} = 0.06$ . Results for piecewise constant and piecewise linear assumptions are shown using both zeroth- and first-order regularization. 224
- Figure 7.18** Optimal estimated heat fluxes using Tikhonov Regularization for triangular test case with  $\Delta\tilde{t} = 0.06$ . Results for piecewise constant and piecewise linear assumptions are shown using both zeroth- and first-order regularization. 226
- Figure 7.19** Optimal estimated heat fluxes using Tikhonov Regularization for quartic test case with  $\Delta\tilde{t} = 0.06$ . Results for piecewise constant and piecewise linear assumptions are shown using both zeroth- and first-order regularization. 226
- Figure 7.20** Filter coefficients for Tikhonov Regularization obtained from temperature perturbation case with  $\Delta\tilde{t} = 0.06$  using either piecewise constant or piecewise linear assumptions with either zeroth- or first-order regularization. Optimal values for regularization coefficient shown for triangular test case using noisy data with  $\sigma_{noise} = 0.5\% \times T_{max}$ . 227
- Figure 7.21** Filter coefficients for Tikhonov Regularization with  $\Delta\tilde{t} = 0.03$  using piecewise constant heat flux assumption with zeroth-order regularization for a range of regularization coefficients. 228
- Figure 7.22** Filter coefficients for Tikhonov Regularization with  $\Delta\tilde{t} = 0.03$  using piecewise linear heat flux assumption with first-order regularization for a range of regularization coefficients. 228
- Figure 7.23** Optimal estimated heat fluxes using Conjugate Gradient Method for step change test case with  $\Delta\tilde{t} = 0.06$ . Results for piecewise constant and piecewise linear assumptions are shown using both Steepest Descent and Fletcher-Reeves methods. 229
- Figure 7.24** Optimal estimated heat fluxes using conjugate gradient method for triangular test case with  $\Delta\tilde{t} = 0.06$ . Results for piecewise constant and piecewise linear assumptions are shown using both Steepest Descent and Fletcher-Reeves methods. 230
- Figure 7.25** Optimal estimated heat fluxes using conjugate gradient method for quartic test case with  $\Delta\tilde{t} = 0.06$ . Results for piecewise constant and piecewise linear assumptions are shown using both Steepest Descent and Fletcher-Reeves methods. 231
- Figure 7.26**  $E(R_q^2)$  versus iteration number for Steepest Descent in the triangular heat flux test case with  $\Delta\tilde{t} = 0.060$ . Optimal  $E(R_q^2)$  indicated with a plus “+” marker. 232
- Figure 7.27**  $E(R_q^2)$  versus iteration number for Fletcher-Reeves CGM in the triangular heat flux test case with  $\Delta\tilde{t} = 0.060$ . Optimal  $E(R_q^2)$  indicated with a diamond marker. 232
- Figure 7.28** Filter coefficients for conjugate gradient methods obtained from temperature perturbation case with  $\Delta\tilde{t} = 0.06$  using either piecewise constant or piecewise linear assumptions using either Steepest Descent (SD) or Fletcher-Reeves (FR) iterations. Optimal number of iterations shown for quartic test case using noisy data with  $\sigma_{noise} = 0.5\% \times T_{max}$ . 233
- Figure 7.29** Filter coefficients for Steepest Descent iterations with  $\Delta\tilde{t} = 0.03$  using piecewise constant heat flux assumption for increasing number of iterations  $n_{iter}$ . 233



- Figure 7.30** Filter coefficients for Fletcher-Reeves Conjugate Gradient iterations with  $\Delta\tilde{t} = 0.03$  using piecewise constant heat flux assumption for increasing number of iterations  $n_{iter}$ . 234
- Figure 7.31** Optimal estimated heat fluxes using Truncated Singular Value Decomposition for step change test case with  $\Delta\tilde{t} = 0.06$ . Results for piecewise constant and piecewise linear assumptions are shown. 235
- Figure 7.32** Optimal estimated heat fluxes using Truncated Singular Value Decomposition for triangular test case with  $\Delta\tilde{t} = 0.06$ . Results for piecewise constant and piecewise linear assumptions are shown. 236
- Figure 7.33** Optimal estimated heat fluxes using Truncated Singular Value Decomposition for quartic test case with  $\Delta\tilde{t} = 0.06$ . Results for piecewise constant and piecewise linear assumptions are shown. 236
- Figure 7.34** Filter coefficients for Truncated SVD method with  $\Delta\tilde{t} = 0.06$  using either piecewise constant or piecewise linear assumptions. Optimal number of singular values to remove shown for quartic test case using noisy data with  $\sigma_{noise} = 0.5\% \times T_{max}$ . 237
- Figure 7.35** Filter coefficients for Truncated SVD with  $\Delta\tilde{t} = 0.03$  using piecewise constant heat flux assumption for increasing number of removed eigenvalues  $n_{sing}$ . 238
- Figure 7.36**  $E(R_q^2)$  and its random and bias error components as  $n_{sing}$  is increased for Truncated SVD with  $\Delta\tilde{t} = 0.060$  using piecewise constant heat flux assumption with the quartic heat flux test case. 238
- Figure 7.37** Optimal estimated heat fluxes using Kalman Filter for step change test case with  $\Delta\tilde{t} = 0.06$ . 240
- Figure 7.38** Optimal estimated heat fluxes using Kalman Filter for triangular test case with  $\Delta\tilde{t} = 0.06$ . 240
- Figure 7.39** Optimal estimated heat fluxes using Kalman Filter for quartic test case with  $\Delta\tilde{t} = 0.06$ . 241
- Figure 7.40** Filter coefficients for Kalman Filter solution with  $\Delta\tilde{t} = 0.06$  optimized with the step heat flux test case. 242
- Figure 7.41** Filter coefficients for Kalman Filter solution with  $\Delta\tilde{t} = 0.06$  optimized with the triangular heat flux test case. 242
- Figure 7.42** Filter coefficients for Kalman Filter solution with  $\Delta\tilde{t} = 0.06$  and  $r = 0$  (no smoothing) showing effect of the regularizing process noise parameter  $Q_q$ . 242
- Figure 7.43** Filter coefficients for Kalman Filter solution with  $\Delta\tilde{t} = 0.06$  and  $Q_q = 68.3$  (optimal for triangular with  $\Delta\tilde{t} = 0.060$ ) showing effect of the smoothing parameter  $r$ . 243
- Figure 7.44** Estimated and exact heat fluxes for Example 7.1. 244
- Figure 8.1** Schematic of a rectangular domain, partially heated from the bottom surface. 250
- Figure 8.2** Schematic of partial heating of a rectangular plate from the bottom surface. 250
- Figure 8.3** Schematic of an IHCP with four unknown heat fluxes and four temperature sensors. 250
- Figure 8.4** Rows of the filter matrix for Example 8.1 ( $\alpha_t = 10^{-4}$  and  $\alpha_s = 10^{-5}$ , dimensionless time step: 0.05). 252
- Figure 8.5** Filter coefficients for Example 8.1 ( $\alpha_t = 10^{-4}$  and  $\alpha_s = 10^{-5}$ , dimensionless time step: 0.05). 253
- Figure 8.6** Input surface heat fluxes for Example 8.1 254
- Figure 8.7** Temperature data at four locations for Example 8.1. 254
- Figure 8.8** Estimated surface heat flux values for Example 8.1 ( $q_1, q_2, q_3$ , and  $q_4$ ). 255
- Figure 8.9** Estimated heat flux values for Example 8.1 in the presence of 0.5% error in temperature data. 256
- Figure 8.10** Heat fluxes applied on the bottom surface of the domain (Example 8.2). 256
- Figure 8.11** Calculated temperatures for the sensors at different locations (Example 8.2). 257
- Figure 8.12** Filter coefficients for Example 8.2 ( $\alpha_t = 10^{-4}$  and  $\alpha_s = 10^{-5}$  and dimensionless time step  $\Delta\tilde{t} = 0.05$ ). 257
- Figure 8.13** Estimated heat flux values for Example 8.2 with 0.5% error present in the temperature data ( $q_1, q_2, q_3$ , and  $q_4$ ). 258
- Figure 8.14** Schematic of an IHCP with two unknown heat fluxes and two temperature sensors (Problem 8.1). 258
- Figure 9.1** Electrically heated flat plate. 262
- Figure 9.2** Temperatures and sensitivity coefficients for convective heat transfer from a lumped body. 264
- Figure 9.3** Heat transfer coefficient history approximated by constant segments. 264
- Figure 9.4** Heat transfer sensitivity coefficients for  $h_i$  constant over segments and  $h_1 = h_2 = \dots = h_0$  and  $T_{\infty,1} = T_{\infty,2} = \dots T_{\infty}$ . (a)  $\Delta t^+ = 0.25$  and (b)  $\Delta t^+ = 0.50$ . 265
- Figure 9.5** Filter coefficient for zeroth-order Tikhonov regularization for heat flux estimation in Example 9.1. 268
- Figure 9.6** Effect of regularization parameter for zeroth-order Tikhonov on heat transfer estimates in Example 9.1. 269
- Figure 9.7** Estimate heat transfer coefficients for Example 9.5 for various regularization parameters. Dashed line indicates the exact values. 274

- Figure 10.1** Isotherms around an idealized temperature sensor: (a) sensor imbedded in low conductivity domain and (b) intrinsic thermocouple on metal surface. 278
- Figure 10.2** Schematic of idealized subsurface thermocouple installation and nomenclature of Beck (1968) and Woolley and Woodbury (2008). 279
- Figure 10.3** ANSYS mesh and typical simulation results. 281
- Figure 10.4** Correction kernel  $\mathbf{H}$  for various regularization coefficients. 282
- Figure 10.5** Heat flux and reconstructions for varying values of  $\alpha_{Tik}$  in Example 10.2. 283
- Figure 10.6** Measured and corrected sensor readings in Example 10.3 using exact data. 285
- Figure 10.7** Measured and corrected sensor readings in Example 10.3 using noisy data with  $\sigma_{noise} = 1.0$  K. 285
- Figure 10.8** Three-dimensional geometry used by Woolley et al. (2008). 286
- Figure 10.9** Comparison of axisymmetric and three-dimensional sensor models: (a) calculated temperatures and (b) resulting apparent errors. 286
- Figure 10.10** Intrinsic thermocouple geometry. 288
- Figure 10.11** Temperatures for Example 10.4. 289
- Figure 10.12**  $\mathbf{H}$  vector for Example 10.4. 290
- Figure 10.13** Simulated measurements and corrected temperatures for Example 10.5. 291
- Figure C.1** Principle of superposition applied to the constant surface temperature-rise component  $\theta_{0,i}(t)$  over the time interval  $t = (i - 1)\Delta t \rightarrow i\Delta t$  defined by Eq. (C.5) and shown in Fig. 3.2: (a)  $\theta_{0,i}^{(a)}(t)$  with  $t \in [(i - 1)\Delta t, \infty)$ ; and (b)  $\theta_{0,i}^{(b)}(t)$  with  $t \in [i\Delta t, \infty)$ . 310
- Figure C.2** Principle of superposition applied to the linear-in-time surface temperature rise component  $\theta_{0,i}(t)$  defined by Eq. (3.25) and shown in Figure 3.4: (a)  $\theta_{0,i}^{(a)}(t)$  with  $t \in [(i - 1)\Delta t, \infty)$  defined by Eq. (C.9a); and (b)  $\theta_{0,i}^{(b)}(t)$  with  $t \in [i\Delta t, \infty)$  defined by Eq. (C.9b). 311
- Figure C.3** Basic functions deriving from superposition applied to the linear-in-time function  $\theta_{0,i}^{(a)}(t)$  of Figure C2.a, with  $t \geq (i - 1)\Delta t$ : (a) constant; and (b) linear. 312
- Figure C.4** Basic functions deriving from superposition applied to the linear-in-time function  $\theta_{0,i}^{(b)}(t)$  of Figure C.2b, with  $t \geq i\Delta t$ : (a) constant; and (b) linear. 313

## Nomenclature

<b>1</b>	vector of all ones
<i>a</i>	a constant
<i>A</i>	counting integer for number of decimal places of precision in building block solution (–)
<b>A,B,C</b>	coefficient matrices from numerical discretization of heat conduction equation
<i>b</i>	a constant
<i>Bi</i>	Biot number, $hL/k$ (–)
<i>c</i>	specific heat capacity ( $\text{J kg}^{-1}\text{K}^{-1}$ )
<i>C</i>	volumetric heat capacity, $\rho c$ ( $\text{J m}^{-3}\text{K}^{-1}$ )
<code>ceil(.)</code>	MATLAB function that rounds the argument to the nearest integer greater than or equal to it (–)
<i>d</i>	deviation distance (m)
$\tilde{d}$	dimensionless deviation distance, $d/L$ (–)
$D_M^2$	square of deterministic error for a single heat flux (Eq. 6.13)
<i>E</i>	relative error based on maximum temperature variation (–)
<i>E(.)</i>	expected value operator
<i>E</i>	depth, $0 < E < L$ (m)
$E_{q,\text{bias}}^2$	square of the expected value of the bias error
$E_{q,\text{rand}}^2$	square of the expected value of the random (variance) error
$E_{q,\text{RMS}}$	root mean squared (RMS) error
<i>f</i>	filter coefficient
<i>f(.)</i>	arbitrary function
<i>F</i>	eigenfunction (–)
<b>F</b>	filter matrix
<i>Fo</i>	Fourier number, $\alpha t/L^2$ (–)
<i>g</i>	filter coefficients (Chapter 5)
<i>g(.)</i>	arbitrary function
<i>G</i>	one-dimensional Green's function ( $\text{m}^{-1}$ )
<b>G</b>	filter matrix (X12 case in Chapter 5)
<i>h</i>	heat transfer coefficient ( $\text{W m}^{-2}\text{K}^{-1}$ )
<i>H(.)</i>	Heaviside unit step function (–)
<i>H</i>	temperature correction kernel (Chapter 10) (–)
<b>H</b>	vector of temperature correction kernel values (–)
<b>H<sub>i</sub></b>	discrete Tikhonov regularization matrix ( $i = 0,1,2$ )
<i>i</i>	counting integer for time steps (–)
<b>I</b>	identity matrix
<i>j</i>	counting integer for space steps (–)
<i>k</i>	thermal conductivity ( $\text{W m}^{-1}\text{K}^{-1}$ )
<i>J</i>	number of sensors
<i>K</i>	gain coefficients in Future Times regularization
<b>K</b>	Kalman gain matrix

$L$	length (m)
$\mathcal{L}(\cdot)$	Laplace transform operator
$m$	counting integer in the $x$ -direction (–)
$m_f$	number of required data points from future time steps for filter form solutions
$m_{\max}$	maximum number of terms in summations along $x$ (–)
$m_p$	number of required data points from previous time steps for filter form solutions
$M$	$M$ -th time step and maximum number of time steps (–); constant in Eq. (4.7)
$n$	counting integer in the $y$ -direction; also number of data points (–)
$n_p$	number of pulses
$n_{\max}$	maximum number of terms in summations along $y$ (–)
$N$	$N$ -th space step; also maximum number of steps or times (–)
$p$	power-law exponent (–)
$P$	constant in Eq. (4.8)
$\mathbf{P}$	covariance matrix in Kalman filter solution
$q$	heat flux ( $\text{W m}^{-2}$ )
$\tilde{q}$	dimensionless heat flux, $q/q_0$ (–)
$\mathbf{q}, \mathbf{q}_0$	vector of surface heat-flux components/values ( $\text{W m}^{-2}$ )
$Q^2$	process noise variance
$r$	number of future times
$R^2$	measurement noise variance
$R_q^2$	mean squared error for vector of heat flux estimates (Eq. 6.9)
$R_q$	root mean squared error of heat flux estimates, $R_q = \sqrt{R_q^2}$
$R_T^2$	mean squared error for vector of measured temperature estimates (Eq. 6.36)
$R_M^2$	mean squared error of a single heat flux value
$s$	an integer
$s_q$	standard error
$S$	total number of terms in the computational analytical solution
$S$	sum of squared errors, e.g. $(\mathbf{Y}-\mathbf{T})^T(\mathbf{Y}-\mathbf{T})$
$\mathbf{S}$	measurement covariance in Kalman filter solution
$t$	time (s)
$\tilde{t}$	dimensionless time, $\alpha t/L^2$ (–)
$T$	temperature (K)
$\tilde{T}$	dimensionless temperature, $(T - T_{in})/(T_0 - T_{in})$ or $(T - T_{in})/(q_0 L/k)$ in Chapter 2 (–)
$\mathbf{T}$	vector of temperatures (K)
$\text{tr}[\cdot]$	trace of a matrix
$u$	cotime, $t - \tau$ (s)
$u_i$	random error with zero mean and unity standard deviation
$\mathbf{v}$	measurement noise vector
$V(\cdot)$	variance operator
$V_\alpha$	the GCV function (Eq. 6.49)
$\mathbf{w}^k$	descent direction for iteration $k$ in conjugate gradient method
$\mathbf{w}$	process noise vector
$W$	width (m)
$\tilde{W}$	aspect ratio, $W/L$ (–)
$W_0$	width of “active” (heated or cooled) boundary (m)
$\tilde{W}_0$	dimensionless width of “active” boundary, $W_0/L$ (–)
$x$	rectangular space coordinate (m)
$\tilde{x}$	dimensionless rectangular space coordinate, $x/L$ (–)
$x'$	dummy variable for space (m)
$X$	sensitivity coefficient

$X_{M,i}$	heat flux-based sensitivity coefficient, $\partial T_M(x)/\partial q_{0,i}$ ( $^{\circ}\text{C m}^2 \text{ W}^{-1}$ )
$X_{M,i,j}$	heat flux-based sensitivity coefficient, $\partial T_M(x, y)/\partial q_{0,i,j}$ ( $^{\circ}\text{C m}^2 \text{ W}^{-1}$ )
$\mathbf{X}$	matrix of sensitivity coefficients $X_{M,i}$ (1D case) and $X_{M,i,j}$ (2D case) ( $^{\circ}\text{C m}^2 \text{ W}^{-1}$ )
$\mathbf{X}_0$	vector of sensitivity coefficients $X_{M,0} = \partial T_M/\partial q_{0,0}$ for $q_{0,0}$ (Chapter 3) ( $^{\circ}\text{C m}^2 \text{ W}^{-1}$ )
$\mathbf{X}_0$	matrix of sensitivity coefficients evaluated at surface $x = 0$ (Chapter 10) ( $^{\circ}\text{C m}^2 \text{ W}^{-1}$ )
$y$	rectangular space coordinate (m)
$\tilde{y}$	dimensionless rectangular space coordinate, $y/L$ (—)
$Y$	measured temperature ( $^{\circ}\text{C}$ )
$\mathbf{Y}$	vector of measured temperatures ( $^{\circ}\text{C}$ )
$\mathbf{y}$	vector of measured temperatures by a second sensor on the remote boundary ( $^{\circ}\text{C}$ )
$Z_h$	step sensitivity for heat transfer coefficient (Chapter 9) ( $\text{m}^2 \text{ }^{\circ}\text{C}^2 \text{ W}^{-1}$ )
$\mathbf{Z}$	vector of step sensitivity coefficients for $h$ ( $\text{m}^2 \text{ }^{\circ}\text{C}^2 \text{ W}^{-1}$ )
$\mathbf{Z}$	sensitivity matrix for measured temperature boundary condition at remote boundary (Chapter 5)

## Greek Symbols

$\alpha$	thermal diffusivity, $k/C$ ( $\text{m}^2\text{s}^{-1}$ )
$\alpha_i$	Tikhonov regularization coefficient ( $i = 0, 1, 2$ )
$\alpha_T$	Tikhonov regularization parameter for the time term (Chapter 8)
$\alpha_s$	Tikhonov regularization parameter for the space term (Chapter 8)
$\beta$	eigenvalue in the $x$ -direction; also a parameter (—)
$\beta$	ratio of thermal properties (Eq. 10.20)
$\boldsymbol{\beta}$	vector of parameters
$\delta(\cdot)$	Dirac delta function
$\delta$	level of error in measured temperatures for Morozov discrepancy principle
$\gamma$	temperature rise per unit linear-in-time increase of surface heat-flux at $x = 0$ (with $x = L$ kept insulated) over the time $t_{ref} = \Delta t$ , that is, $\tilde{T}_{X22B20T0} \times L/k$ with $\tilde{t}_{ref} = \Delta \tilde{t}$ ( $^{\circ}\text{C m}^2 \text{ W}^{-1}$ )
$\Gamma$	input gain in Kalman filter
$\Delta$	variation of a function (e.g. $\Delta T$ is the variation of the temperature function)
$\Delta\gamma_i$	forward difference of the $\gamma$ temperature at time $i\Delta t$ , $\gamma_{i+1} - \gamma_i$ ( $^{\circ}\text{C m}^2 \text{ W}^{-1}$ )
$\Delta t$	time step (s)
$\Delta \tilde{t}$	dimensionless time step, $\alpha\Delta t/L^2$ (—)
$\Delta y$	space step along $y$ (m)
$\Delta \tilde{y}$	dimensionless space step along $y$ , $\Delta y/L$ (—)
$\Delta\phi_i$	forward difference of the $\phi$ temperature at time $i\Delta t$ , $\phi_{i+1} - \phi_i$ ( $^{\circ}\text{C m}^2 \text{ W}^{-1}$ )
$\Delta\varphi_i$	forward difference of the $\varphi$ temperature at time $i\Delta t$ , $\varphi_{i+1} - \varphi_i$ (—)
$\Delta(\Delta\gamma)_i$	central difference of the $\gamma$ temperature at time $i\Delta t$ , $\Delta\gamma_i - \Delta\gamma_{i-1}$ ( $^{\circ}\text{C m}^2 \text{ W}^{-1}$ )
$\Delta_i\lambda$	forward difference at time $i\Delta t$ of the $\lambda$ temperature, $\lambda_{i+1} - \lambda_i$ ( $^{\circ}\text{C m}^2 \text{ W}^{-1}$ )
$\Delta_j\lambda$	backward difference at the $j$ -th grid point of the $\lambda$ temperature, $\lambda_j - \lambda_{j-1}$ ( $^{\circ}\text{C m}^2 \text{ W}^{-1}$ )
$\Delta_i\Delta_j(\lambda)$	second cross difference in space ( $\Delta_j$ ) and time ( $\Delta_i$ ) at the $j$ -th grid point and at time $i\Delta t$ of the $\lambda$ temperature, $\Delta_j(\lambda_{i+1}) - \Delta_j(\lambda_i) = \Delta_j\Delta_i(\lambda)$ ( $^{\circ}\text{C m}^2 \text{ W}^{-1}$ )
$\Delta\mu_i$	forward difference of the $\mu$ temperature at time $i\Delta t$ , $\mu_{i+1} - \mu_i$ (—)
$\Delta(\Delta\mu)_i$	central difference of the $\mu$ temperature at time $i\Delta t$ , $\Delta\mu_i - \Delta\mu_{i-1}$ (—)
$\varepsilon_a$	absolute error ( $^{\circ}\text{C}$ )
$\varepsilon_r$	relative error (—)
$\varepsilon_i$	a single random error
$\boldsymbol{\varepsilon}$	vector of random error
$\eta$	eigenvalue in the $y$ -direction (—)
$\nabla$	gradient operator

$\nabla_{\mathbf{q}}$	gradient with respect to the components of vector $\mathbf{q}$
$\theta_0$	surface temperature rise, $T_0(t) - T_{in}$ (K)
$\boldsymbol{\theta}_0$	vector of surface temperature-rise components/values ( $^{\circ}\text{C}$ )
$\lambda$	temperature rise per unit of surface heat flux of the X22B(y1pt1)0Y22B00T0 heat conduction case, that is, $\tilde{T}_{\text{X22B(y1pt1)0Y22B00T0}} \times L/k$ ( $^{\circ}\text{C m}^2 \text{ W}^{-1}$ )
$\Lambda_j$	heat flux-based sensitivity coefficient, $\partial T(x,y,t)/\partial q_{0,j}$ ( $^{\circ}\text{C m}^2 \text{ W}^{-1}$ )
$\mathbf{\Lambda}$	vector of sensitivity coefficients $\Lambda_j$ ( $^{\circ}\text{C m}^2 \text{ W}^{-1}$ )
$\mu$	temperature rise per unit linear-in-time increase of surface temperature at $x = 0$ being $x = L$ insulated over the time $t_{ref} = \Delta t$ , that is, $\tilde{T}_{\text{X12B20T0}}$ with $\tilde{t}_{ref} = \Delta \tilde{t}$ (—)
$\rho$	density ( $\text{kg m}^{-3}$ )
$\rho^k$	descent direction on iteration $k$ for conjugate gradient method
$\sigma$	standard deviation
$\tau$	dummy variable for time (s)
$\phi$	temperature rise per unit step change of surface heat flux at $x = 0$ with $x = L$ kept insulated, that is, $\tilde{T}_{\text{X22B10T0}} \times L/k$ ( $^{\circ}\text{C m}^2 \text{ W}^{-1}$ )
$\phi(.)$	generic influence function – response in domain due to step change in surface condition
$\Phi$	state transition matrix
$\varphi$	temperature rise per unit step change of surface temperature at $x = 0$ being $x = L$ insulated, that is, $\tilde{T}_{\text{X12B10T0}}$ (—)
$\psi$	Lagrange multiplier
$\Psi_{M,i}$	temperature-based sensitivity coefficient, $\partial T_M(x)/\partial \theta_{0,i}$
$\Psi$	matrix of sensitivity coefficients $\Psi_{M,i}$ for $\boldsymbol{\theta}_0$ (—)
$\Psi_0$	vector of sensitivity coefficients $\Psi_{M,0} = \partial T_M(x)/\partial \theta_{0,0}$ for $\theta_{0,0}$ (—)

## Subscripts

0	boundary surface at $x = 0$ ; also, initial time $t = 0$
$\infty$	undisturbed fluid
$\alpha$	pertaining to regularization (Tikhonov or other)
$b$	body
$c$	computational
$c$	constant
$ct$	complementary transient
$d$	deviation
$\delta$	second deviation
$e$	exact
$f$	final time
$i$	$i$ -th time step; also, $i$ -th component in time of surface temperature or surface heat flux
$j$	$j$ -th space step ( $y_N = W$ ); also, $j$ -th component in space of surface heat flux
$in$	initial (time $t = 0$ )
$L$ -curve	pertaining to the $L$ -curve (Section 6.6)
$m$	counting integer in the $x$ -direction
$M$	$M$ -th time step
$n$	counting integer in the $y$ -direction
$n_s$	number of singular values removed in TSVD
$N$	$N$ -th space step
$opt$	optimal
$p, pen$	penetration time (Eq. 4.1)
$p$	“look-ahead” time, $p = r_{opt}\Delta t$ (Chapter 7) (s)
$p$	sensor measurement location (Chapter 10)
$qs$	quasi steady
$ref$	reference

<i>ss</i>	steady state
<i>us</i>	unsteady
<i>w</i>	wire
<i>x</i>	along the <i>x</i> –direction
X12	heat conduction along <i>x</i> with BCs of the 1st and 2nd kind
X22	heat conduction along <i>x</i> with BCs of the 2nd kind on both sides
XI0BKT0	heat conduction along <i>x</i> for a semi-infinite body with BC of the 1st kind ( <i>I</i> = 1) or of the 2nd kind ( <i>I</i> = 2); <i>K</i> = 1 or 2 for a constant or linear-in-time BC
<i>y</i>	along the <i>y</i> –direction
<i>Y</i>	pertaining to measurement

## Superscripts

$\sim, +$	dimensionless quantity
$-$	mean or average
$-$	Laplace transform of function (Chapter 10)
$\wedge$	estimated value
$T$	transpose of a matrix
( <i>A</i> )	counting integer for number of decimal places of precision in solution
( <i>L</i> )	large-time form
( <i>S</i> )	short-time form

## Acronyms

1D	one-dimensional
2D	two-dimensional
3D	three-dimensional
BC	boundary condition
BEM	boundary element method
CD	central difference
CGM	conjugate gradient method
DHCP	direct heat conduction problem
FD	forward difference
FR	Fletcher-Reeves conjugate gradient method
FS	function Specification
GF	Green's function
GFSE	Green's function solution equation
IHCP	inverse heat conduction problem
KF	Kalman filter
LHS	left-hand side
LT	Laplace transform
RHS	right-hand side
SD	Steepest Descent iteration method
SOV	separation of variables
SVD	singular value decomposition
TSVD	truncated singular value decomposition
TR	Tikhonov regularization
USEM	unsteady surface element method

## Preface to First Edition

This book presents a study of the inverse heat conduction problem (IHCP), which is the estimation of the surface heat flux history of a heat conducting body. Transient temperature measurements *inside* the body are utilized in the calculational procedure. The presence of errors in the measurements as well as the ill-posed nature of the problem lead to “estimates” rather than the “true” surface heat flux and/or temperature.

This book was written because of the importance and practical nature of the IHCP; furthermore, at the time of writing, there is no available book on the subject written in English. The specific problem treated is only one of many ill-posed problems but the techniques discussed herein can be applied to many others. The basic objective is to estimate a function given measurements that are “remote” in some sense. Other applications include remote sensing, oil exploration, nondestructive evaluation of materials, and determination of the Earth’s interior structure.

The authors became interested in the IHCP over two decades ago while employed in the aerospace industry. One of the applications was the determination of the surface heat flux histories of reentering heat shields.

This book is written as a textbook in engineering with numerical examples and exercises for students. These examples will be useful to practicing engineers who use the book to become acquainted with the problem and methods of solution. A companion book, *Parameter Estimation in Engineering and Science* by J. V. Beck and K. J. Arnold (Wiley 1977), discusses the estimation of certain constants or parameters rather than functions as in the IHCP. Though many of the ideas relating to least squares and sensitivity coefficients are present in both books, the present book does not require a mastery of parameter estimation.

The book is written at the advanced BS or the MS level. A course in heat conduction at the MS level or courses in partial differential equations and numerical methods are recommended as prerequisite materials.

Our philosophy in writing this book was to emphasize general techniques rather than specialized procedures unique to the IHCP. For example, basic techniques developed in Chapter 4 can be applied either to integral equation representations of the heat diffusion phenomena or to finite difference (or element) approximations of the heat conduction equation. The basic procedures in Chapter 4 can treat nonlinear cases, multiple sensors, nonhomogeneous media, multidimensional bodies, and many equations, in addition to the transient heat conduction equation.

The two general procedures that are used are called (a) function specification and (b) regularization. A method of combining these (the trial function method) is also suggested. One of the important contributions of this book is the demonstration that all of these methods can be implemented in a sequential manner. The sequential method in some case gives nearly the same result as whole domain estimation and yet is much more computationally efficient.

One of our goals was to provide the reader with an insight into the basic procedures that provide analytical tools to compare various procedures. We do this by using the concepts of sensitivity coefficients, basic test cases, and the mean squared error. The reader is also shown that optimal estimation involves the compromise between minimum sensitivity to random measurement errors and the minimum bias.

Preliminary notes have been used for an ASME short course and for a graduate course at Michigan State University.

There are many people who have helped in the preparation of this text and to whom we express our appreciation. These include D. Murio, M. Raynaud, other colleagues, and students who have read and commented on the notes. Thanks are also due to Judy Duncan, Phyllis Murph, Terese Stuckman, Alice Montoya, and Jeana Pineau, who have aided in typing the manuscript.

James V. Beck wishes to express appreciation for the contributions to his education made by Kenneth Astill of Tufts University, Warren Rohsenow of Massachusetts Institute of Technology, and A. M. Dhanak of Michigan State University.

Ben Blackwell would like to acknowledge the contributions that several people made to his heat transfer education: H. Wolf of the University of Arkansas, M. W. Wildin of the University of New Mexico, and W. M. Kays of Stanford University.

A special and deep appreciation is extended to George A. Hawkins for the education and philosophy that he imparted to Charles R. St. Clair, Jr. as his graduate student.

James V. Beck  
Ben Blackwell  
Charles R. St. Clair, Jr.  
East Lansing, Michigan  
Albuquerque, New Mexico  
East Lansing, Michigan  
August 1985



## Preface to Second Edition

The first edition of this textbook was published in 1985. At that time, the IBM PC had been available for about four years, and release of the IBM PS/2 was still two years in the future. These historical milestones frame the thinking of the times about computing in the mid-1980s. It is often said, and is demonstrably true, that any common pocket cell phone of the 2020s has significantly more computation and storage capability than early scientific computing machines. While the first edition of the book continues to be used by researchers and professionals as a major reference on inverse heat conduction problems (IHCPs), with the major advancements in solution techniques for IHCPs and the vast progress in use of computer programs for solving engineering problems over the past few decades, the need for writing the second edition of the book was long due.

Over the past 30 years, the authors of this second edition have collaborated on an array of research projects on exact solutions to heat conduction problems and solution of inverse heat conduction problems (IHCPs), and much of that research forms the basis for this book.

This text aims to present the methodology of many IHCP solution techniques (Chapter 4) and outline approaches for optimizing the degree of regularization in an IHCP solution (Chapter 6). These discussions will be presented primarily in the framework of the filter matrix concept presented in Chapter 5.

Almost 40 years have passed since publication of the first edition of this book, and much research on IHCPs and their solutions has been performed since that time. Chapter 1 presents an extensive literature review of IHCP work over the past decades in the areas of manufacturing, aerospace, biomedical, electronics cooling, instrumentation, nondestructive testing, and other areas of engineering applications. Throughout the text, additional references are offered to guide the interested reader to sources for additional information.

Because computing power today is great, many (most?) direct heat conduction problems are solved using commercial software based on finite element or finite difference methodology. However, analytical solutions provide highly accurate results that can be computed efficiently. This second edition continues the emphasis from the first edition on utilization of exact solutions for linear heat transfer problems – those with thermophysical properties that are independent of temperature. Chapter 2 presents exact solutions to several fundamental problems, and superposition of these solutions provides a gateway to solution of a wide array of problems. Also discussed in Chapter 2 is the concept of the computational analytical solution which provides efficient and accurate computation of the solution.

Chapter 3 outlines approximate solution methods for linear problems which form the basis for the IHCP solutions in the remainder of the book. These concepts are presented using ideas of superposition of exact solutions; however, a more rigorous treatment using Green's functions is given in Appendix.

Chapter 4 retains detailed description of the Stolz method, the Function Specification (Beck's) Method, and Tikhonov regularization. New to this second edition are descriptions of the Conjugate Gradient Method and Singular Value Decomposition. Additionally, two methods that are amenable to nonlinear problems are explained: the Adjoint Method, which is used in conjunction with the Conjugate Gradient Method, and the Kalman Filter approach to solving the IHCP.

Chapter 6 is new to the second edition and focuses on selection of the optimal degree of regularization in solution of IHCPs. Because IHCPs are inherently ill-posed, some form of regularization is necessary. Regularization decreases sensitivity to noise in measurements at the expense of introducing bias into the estimates. Striking the appropriate balance between these competing factors is an important, and often overlooked, part of analyzing an IHCP.

Because of the relative costliness of computer resources at the time, a significant focus of the first edition was computational efficiency of IHCP algorithms. In this second edition, more attention is devoted to comparing accuracy of IHCP solution methods than to their computational efficiency. Chapter 7 contains head-to-head comparison of many IHCP solution methods using a common suite of test problems.

The filter coefficient concept is used throughout the text. Chapter 5 explores the nature of the filter matrix for many IHCP methods presented in Chapter 4. The character of many of these filter matrices is such that a truncated filter vector can be extracted from the matrix to use in sequential online (near real-time) estimation. Additionally, Chapter 5 illustrates how linear IHCP concepts can be applied to problems with temperature-dependent thermophysical properties. Chapter 8 outlines application of the filter concepts to two-dimensional transient IHCP problems with multiple unknown heat fluxes.

Chapter 9 addresses the problem of estimating the heat transfer coefficient,  $h$ . Much of the chapter focuses on the case of lumped capacitance bodies (with negligible internal temperature gradients) and outlines several approaches for estimating  $h$  under those conditions. Application to bodies with temperature gradients is also discussed.

Chapter 10 is new to this edition and addresses bias in temperature measurements caused by sensor installation. Two situations are explored: correction of measured temperature to remove the bias and utilization of the biased measurements directly in the IHCP solution. Both situations typically require a computational model which incorporates the sensor in the domain and can be used to quantify the bias.

The second edition of the book also comes with additional materials that are available on a companion website. These materials include MATLAB codes for the examples that are solved in the book. Furthermore, course slides, additional problems, and suggested course syllabus will be available for instructors.

Keith A. Woodbury  
Hamidreza Najafi  
Filippo de Monte  
James V. Beck  
Tuscaloosa, AL, USA  
Melbourne, FL, USA  
L'Aquila, Italy  
East Lansing, MI, USA  
June 2022